Dust charge distribution in a plasma afterglow

I. B. Denysenko[1,2,3], M. Mikikian[2]

[1]*School of Physics and Technology, V. N. Karazin Kharkiv National University, Ukraine*

[2]*GREMI, UMR 7344 CNRS/Université d'Orléans, F-45067 Orléans, France*

[3]*Le Studium, Loire Valley Institute for Advanced Studies, Orléans & Tours, France*

Discharging of dust particles in an argon plasma afterglow was investigated. The study was carried out using different approaches. First, we obtained the dust charge distribution function (DCDF) F_k by solving numerically the master equation [1]:

$$\frac{d}{dt}F_k = \nu_{ed}^{k+1}F_{k+1} - \nu_{ed}^{k}F_k - (\nu_{id}^{k} + \nu_m)F_k + (\nu_{id}^{k-1} + \nu_m)F_{k-1}, \quad (1)$$

where t is the afterglow time, ν_{ed}^{k} and ν_{id}^{k} are the frequencies with which a particle with charge $Z_d^k = ke$ collects electrons and ions, respectively, k is an integer and e is the elementary charge. ν_m is the frequency describing electron emission from the dust surface at collisions of dust particles with argon atoms in excited states. The DCDF is normalized by $\Sigma_k F_k = 1$.

We also calculated the mean dust charge Z_d using the following expression

$$\frac{\partial Z_d}{\partial t} = \nu_{id} + \nu_m - \nu_{ed}, \quad (2)$$

where ν_{id} and ν_{ed} are, respectively, the frequencies describing collection of ions and electrons by a dust particle with the charge Z_d.

We also compared the DCDF calculated from Eq. (1) with the Gaussian distribution [1]:

$$F_{Gk} = \frac{1}{\left(2\pi\sigma_z^2\right)^{1/2}}\exp\left[-\frac{(-Z_d^k + Z_d)^2}{2\sigma_z^2}\right], \quad (3)$$

where Z_d is determined by Eq. (2), and the variance σ_z^2 as a function of time is found from the following equation [1]:

$$\frac{d\sigma_z^2}{dt} \approx -\alpha_1'\sigma_z^2 + \alpha_2, \quad (4)$$

where $\alpha_1' = 2(\nu_{ed}' - \nu_{id}')$ with primes indicating derivatives with respect to Z_d, $\alpha_2 = \nu_{ed} + \nu_{id} + \nu_m$.

Using Eqs. (1) - (4), we calculated the dust charge distribution function, mean dust charge and variance in an argon afterglow plasma, as functions of time. The calculations were

carried out for the plasma with radius R=2 cm and height L=3 cm (the plasma sizes here are the same as in [2]). It was assumed that the plasma contains electrons with density n_e, singly charged positive argon ions with density n_i, ground-state argon atoms with density n_a, metastable argon atoms (Ar_m) with density n_m, argon atoms in the resonance 4s states ($^3P_1$ and $^1P_1$) (Ar_r) with density n_r as well as argon atoms in 4p states (Ar_{4p}) with density n_{4p}. We assumed that at t = 0, $n_e = n_i = 5\times10^9 cm^{-3}$ and that the plasma contains dust particles with density n_d = 5×10^4 cm^{-3}, as in [2], and radius a_d. The results were obtained for different dust radii. The study was carried out taking into account for the transition from ambipolar to free diffusion in the plasma afterglow. The electron diffusion was described in the same manner as in [3], while the ion diffusion as in [4]. The neutral gas pressure was taken to be P = 0.3 Torr, as in [2]. In [5], one can find the results for the P = 0.9 Torr case additionally.

The results were obtained taking into account secondary electron emission in the collisions of excited argon atoms Ar* (Ar_m, Ar_r and Ar_{4p}) with dust particles (for the secondary emission yield γ_m=0.035), as well as neglecting by this process (γ_m =0). Since the value of γ_m is not known for the conditions considered here, we used in our simulations the value leading to a good agreement with experimental data [2]. More details on our model can be found in [5].

Fig. 1 shows that the initial $|Z_d|$ increases if a_d becomes larger, because of larger surface collecting electrons from the plasma volume. The absolute value of mean dust charge decreases faster with time in the beginning of afterglow, if dust size is larger [Fig. 1 (a)], due to larger dust charging time (see Fig. 1 (c) in [3]). Moreover, at late afterglow times, the absolute value of mean dust charge may become larger for smaller a_d [Fig. 1(a)]. In particular, $|Z_d|$ for a_d = 5 nm is larger than the absolute values of mean dust charge for a_d = 10 nm and a_d = 20 nm. This is mainly due to smaller ν_{id} in the a_d = 5 nm case compared with the frequencies in the a_d = 10 nm and a_d = 20 nm cases. Note that the secondary emission in metastable-dust collisions affects more essentially the charge of larger dust particles. At late afterglow times (t =100 ms), $|Z_d|$ is 2.37 (2.37), 4.61(4.56), 3.36(3.2), 3.59(3.2), 6.8(5.17), 10.7(6.04), 16.61(3.24) for a_d = 1 nm, 5 nm, 10 nm, 20 nm, 50 nm, 100 nm, 200 nm at γ_m =0 (γ_m =0.035), respectively. Thus, at t =100 ms and γ_m =0.035, the absolute value of mean dust charge for a_d = 200 nm is smaller than $|Z_d|$ for a_d = 5, 50 and 100 nm because of the secondary emission. It is not the case for γ_m =0.0.

At late afterglow times, the mean charges of dust particles with different a_d may be nearly the same (see $|Z_d(t)|$ in Fig. 1 (a) for a_d = 10 nm, 20 nm and 200 nm), while the variances are very different [Fig. 1 (b)]. Similarly, the variances for different a_d may be nearly the same

(see σ_z^2 in Fig. 1 (b) for a_d = 5 nm and 10 nm), while the mean charges differ essentially [Fig. 1 (a)].

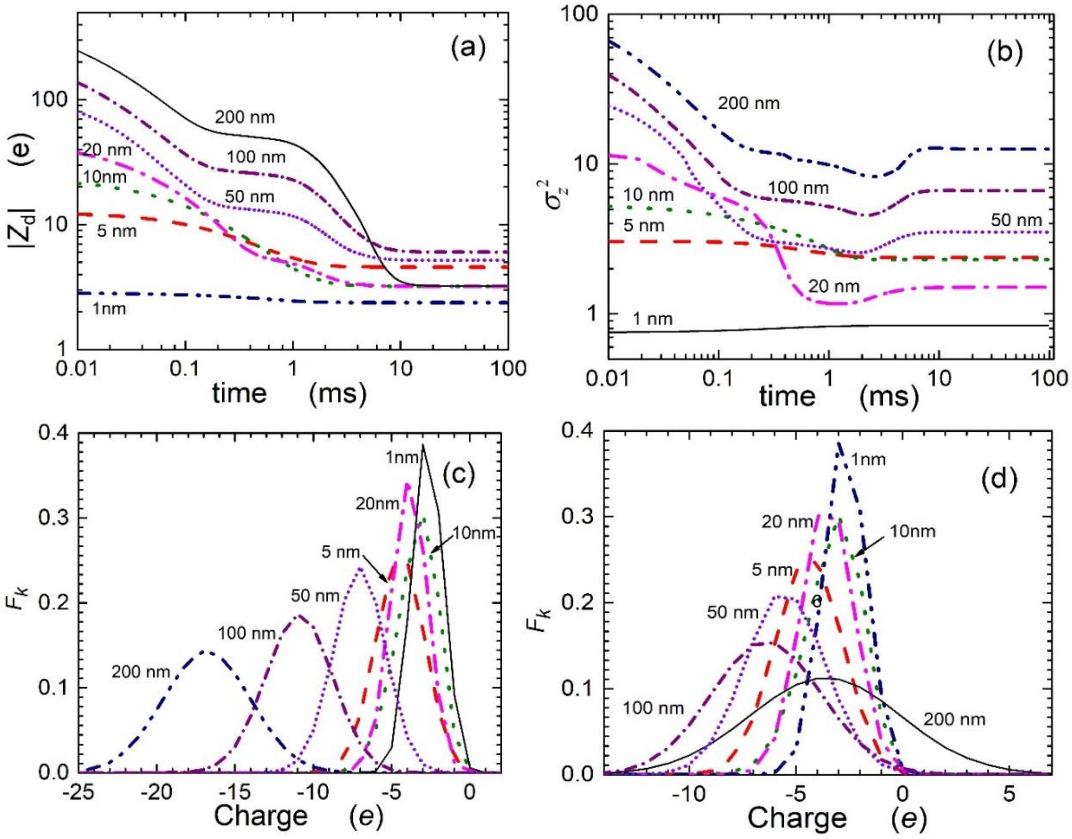

Fig. 1. The mean dust charge (a) and the variance (b) for γ_m =0.035, and the dust charge distribution function obtained from Eq. (1) at t = 100 ms for a_d = 1 nm, 5 nm, 10 nm, 20 nm, 50 nm, 100 nm and 200 nm in the γ_m =0 (c) and γ_m =0.035 (d) cases.

In our opinion, this is due to changing the dust charging time and the variance at a variation of a_d. For large dust particles ($a_d \geq 20$ nm) and $t \geq 0.3$ ms, the variance increases with growth of a_d [Fig. 1 (b)]. This conclusion can be also obtained using the OML approach for the steady-state case at γ_m =0 ($\sigma_z^2 \approx \frac{(1+\nu_{ed}/\nu_{id})a_d T_e}{2e(\tau/(1+\tau|z|)+\nu_{ed}/\nu_{id})} \propto a_d$, where $\tau = T_e/T_i$, T_e and T_i are the electron and ion temperatures, respectively, and $z = eZ_d/a_d T_e$). The variance depends also on γ_m, and at late afterglow times for large dust particles, σ_z^2 in the case of γ_m =0.035 is larger than that in the case of γ_m =0. At t =100 ms, the variance is 0.83 (0.83), 2.34 (2.37), 2.21 (2.3), 1.28 (1.5), 2.67 (3.52), 4.51 (6.65) and 7.66 (12.57) for a_d = 1 nm, 5 nm, 10 nm, 20 nm, 50 nm, 100 nm and 200 nm at γ_m =0 (γ_m =0.035), respectively.

Note that at late afterglow times, most dust particles in the γ_m =0 case are negatively charged, independently on their size [Fig. 1(c)]. In the γ_m =0.035 case, rather large amount of dust particles with a_d = 200 nm are positively charged, while the particles of smaller size are mainly negatively charged. This is due to the fact that for large dust particles, σ_z^2 is larger and $|Z_d|$ is smaller in the γ_m =0.035 case compared with the corresponding values obtained at γ_m =0 [5]. For small a_d ($\leq$ 10 nm), the DCDF in the γ_m =0.035 case is nearly the same as the one obtained for γ_m =0, because σ_z^2 and $|Z_d|$ are also nearly the same in the both cases.

We also calculated the dust charge distribution functions at a_d = 190 nm (as in the experiments [2]) and compared them with the measured DCDF [Fig. 2(a)]. It was found that the calculated DCDF agrees well with the one obtained in experiments [2], if our model accounts for the secondary emission with γ_m = 0.035 [Fig. 2(a)]. At γ_m = 0, the calculated DCDF is shifted to the region of smaller charge (larger $|Z_d|$) compared with the charge distribution function measured in the experiment. The charge distribution calculated from Eq. (1) at γ_m = 0.035 was also compared with the Gaussian distribution obtained using Eqs. (2)- (4). It was found that F_{Gk} approximates rather well the DCDF obtained from the master equation (1) [Fig. 2(b)].

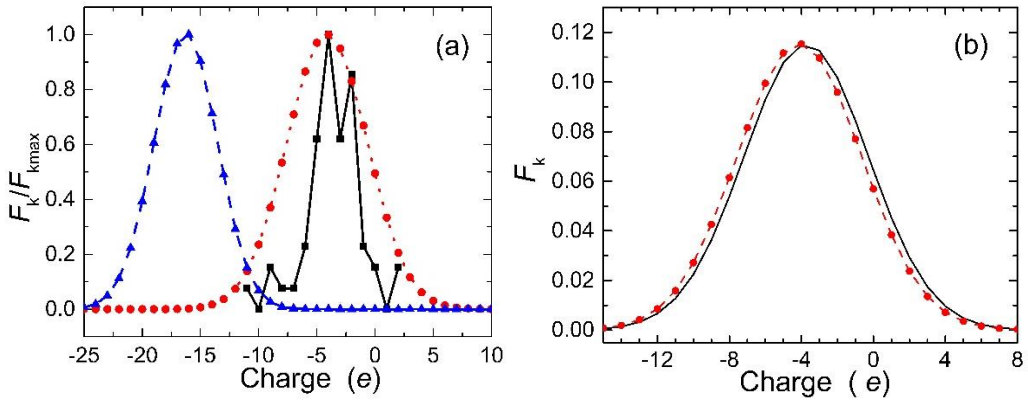

Fig. 2. The normalized DCDFs calculated at t = 100 ms in the γ_m =0 (dashed curve) and γ_m = 0.035 (dotted curve) cases and the DCDF obtained in experiments [2] (solid curve) (a). The dust charge distribution functions calculated at γ_m = 0.035 from Eq. (1) (dashed curve) and the Gaussian distribution obtained from Eq. (3) (solid curve). Here, a_d =190 nm and $F_{k\,max}$ corresponds to the DCDF maximum.

[1] Shotorban B 2011 *Phys. Rev. E* **83**, 066403

[2] Couëdel L, Samarian A A, Mikikian M and Boufendi L 2008 *Phys. Plasmas* **15,** 063705

[3] Denysenko I B, Mikikian M and Azarenkov N A 2022 *J. Phys. D* **55**, 095201

[4] Gerber R A and Gerardo J B 1973 Phy*s. Rev. A* **7**, 781

[5] Denysenko I B, Mikikian M and Azarenkov N A 2022 *Phys. Plasmas*, submitted